Ultrasound-assisted Extraction and Physicochemical Properties of Starch from *Cyperus esculentus* Tubers

Fanhao Meng,[a,b] Shuangqi Tian,[a,b,c,*] Ya'nan Wang,[a,b] Jing Lu,[d] Zehua Liu,[a,b,c] and Yongwu Niu [a,b,c]

**Corresponding author: tianshuangqi2002@126.com*

DOI: 10.15376/biores.19.3.4264-4277

GRAPHICAL ABSTRACT

Ultrasound-assisted Extraction and Physicochemical Properties of Starch from *Cyperus esculentus* Tubers

Fanhao Meng,[a,b] Shuangqi Tian,[a,b,c,*] Ya'nan Wang,[a,b] Jing Lu,[d] Zehua Liu,[a,b,c] and Yongwu Niu [a,b,c]

The purpose of this study was to use ultrasound-based extraction to prepare starch from the tubers of *Cyperus esculentus*. Ultrasonic treatment of *Cyperus esculentus* powder with a medium of alkaline-treated water can effectively improve the starch extraction efficiency. Box-Behnken design was used to optimize the extraction process, and the results showed that the optimal parameters were ultrasound time of 30 minutes, pH value of 9.0, ultrasound temperature of 40 °C, and solid-liquid ratio of 10:1. The extraction percentage under these conditions was 90.1%. The physicochemical properties of *C. esculentus* starch were compared with those of cassava, potato, and corn starch. The particle size of *C. esculentus* starch was approximately 2 to 15 μm. The gelatinization temperature was 70.5 °C, and the peak viscosity was similar to cassava but with better thermal stability. Like other tuber starches, *C. esculentus* starch had higher swelling power and solubility at 85 °C.

DOI: 10.15376/biores.19.3.4264-4277

Keywords: Starch; Cyperus esculentus; Ultrasound-assisted extraction; Physicochemical Properties

*Contact information: a: National Engineering Research Center of Wheat and Corn Further Processing, Henan University of Technology, Zhengzhou 450001, China; b: College of Food Science and Technology, Henan University of Technology, Zhengzhou, 450001, China; c: Food Laboratory of Zhongyuan, Luohe, 462300, China; d: Department of Molecular Sciences, Swedish University of Agricultural Sciences, PO Box 7015, SE-75007 Uppsala, Sweden; *Corresponding author: tianshuangqi2002@126.com*

INTRODUCTION

Cyperus esculentus belongs to the perennial herbaceous plants of the Cyperaceae family in the Poaceae order. *Cyperus esculentus* is native to the Mediterranean region and widely distributed in tropical and subtropical regions around the world. In many countries, *C. esculentus* is present as harmful weeds, often competing with crops and horticultural plants for land resources (Manek *et al.* 2012). In fact, *C. esculentus* tubers contain many beneficial ingredients, and are rich in oil and starch. Studies have reported that their approximate contents of ash, crude fat, crude protein, crude fiber, and carbohydrates were 2.6%, 22.1%, 4.3%, 15.5%, and 48.1%, respectively. Starch is the main component of carbohydrates and its dry basis yield was 20.5% (Adel *et al.* 2015; Codina-Torrella *et al.* 2015). Making *C. esculentus* tubers into beverages is one of the interesting and mainstream application methods. In Spain, *C. esculentus* tubers are used to produce a plant-based milk substitute called "horchita de chufa" (Sánchez-Zapata *et al.* 2012). Aydar *et al.* (2020) conducted a detailed analysis on the production process, bioavailability, and market share of *C. esculentus* and other plant-based dairy substitutes. Recent studies have shown that adding polysaccharide extracts from *C. esculentus* to protein drinks exhibits better stability

than regular protein drinks (Yu *et al*. 2023). Chukwuma *et al.* (2010) observed the presence of alkaloids, cyanosides, resins, tannins, sterols, and saponins in the raw *C. esculentus* tubers, confirming that the tubers contain important nutrients and are essential nutrients for human health.

The starch content of *C. esculentus* tubers is high. Wu *et al*. (2024) analyzed the starch composition of *C. esculentus* from six different regions in China, with the highest starch content reaching 34.8%. Sometimes people use cold pressing to obtain the oil of *C. esculentus* tubers, while the remaining oil residue cake is used for feed, and the starch in it is not well utilized. Extracting starch from the oil residue cake of *C. esculentus* tubers is a potential way to improve its utilization efficiency. In recent years, ultrasound treatment has been increasingly applied in starch extraction, resulting in varying degrees of improvement in starch yield (Liu *et al.* 2020; Wang *et al.* 2022; Mieles-Gómez *et al.* 2023). The mechanism of ultrasound-assisted extraction is explained as the interaction between ultrasound and sound fields, causing cavitation bubbles in the liquid. The generation and disappearance of cavitation bubbles cause local pressure changes, resulting in turbulence, microjets, and shear effects (Cárcel *et al.* 2012). These effects can cause cell wall rupture, enhance the separation and dissolution of various biochemical components, such as promoting the separation of starch from lipids, proteins, and fibers, thereby improving the starch extraction yield.

This study used ultrasound-assisted extraction of starch and explored the optimal process conditions with extraction yield as the evaluation index. Through conducting scanning electron microscopy (SEM), differential scanning calorimetry (DSC), and rapid viscosity determination (RVA) analyses, as well as examining the solubility and swelling power, the extracted *C. esculentus* starch, commodity cassava, potato, and corn starch were studied to gain a deeper understanding of the physicochemical properties of *C. esculentus* starch.

EXPERIMENTAL

Materials

Cyperus esculentus tubers were produced in Shaoyang City, Hunan Province (Hunan, China). N-hexane and anhydrous ethanol were purchased from Fuyu Chemical Co., Ltd. (Tianjin, China). Hydrochloric acid was purchased from Kermel Chemical Co., Ltd. (Tianjin, China). Cassava, potato, and corn starch were purchased from Xinxiang Xinliang Grain and Oil Processing Co., Ltd. (Henan, China).

Defatting Treatment of *C. esculentus* Tubers

Fresh *C. esculentus* tubers were cleaned and oven-dried at 45 °C for 24 h to reduce moisture content. A universal crusher (YIRUI FW100, Tianjin Taisite Instrument Co., Ltd., Tianjin, China) was used to crush them to a size that could pass through a 20-mesh sieve. Material was processed through a hydraulic oil press (6YY-220, Luofeng Hydraulic Technology Co., Ltd., Henan, China) to obtain *C. esculentus* oil residue cake. The cake was crushed to pass through a 40-mesh sieve, and then n-hexane was used as a defatting treatment with solid-liquid ratio 6:1 for 5 h. After the n-hexane was filtered out, clean n-hexane was added for secondary defatting of *C. esculentus*. The solid-liquid ratio at this time was 3:1 for 5 h. Then, the n-hexane was filtered out again. The obtained secondary defatted *C. esculentus* was dried at 45 °C for 12 h and processed by a crushing method

once more to a particle size of about 60-mesh and the *C. esculentus* defatted powder was obtained.

Extraction of Starch

Extraction of starch was achieved using the ultrasound-assisted alkaline method. Sodium hydroxide solution with a certain pH was mixed with *C. esculentus* defatted powder at a certain solid-liquid ratio and placed in a conical flask. The conical flask was placed into an ultrasonic water bath device with temperature control function (KQ5200DE, Kun Shan Ultrasonic Instruments Co., Ltd., Jiangsu, China), and the ultrasonic power was 200 W. After treatment at a certain temperature for a desired period of time, the material structure became loose under the ultrasonic effect, and the degree of binding between different components was reduced, thereby improving the efficiency of starch separation. After ultrasonic treatment, magnetic stirring (RCT basic, IKA Instrument and Equipment Co., Ltd., Germany) was performed for 30 min to fully dissolve the protein and other soluble substances in the *C. esculentus*. Afterwards, it was centrifuged (5810-R, Eppendorf AG, Germany) at 4000 rpm for 15 min, the supernatant was poured out. The precipitate was washed with distilled water, passed through a 200-mesh sieve, and the sieved material was centrifuged again and washed with water. After three repetitions, the precipitate was labelled as the extracted starch. It was washed with 80% alcohol and dried at 45 °C for 24 h. The obtained starch was crushed to pass through a 100-mesh sieve to obtain *C. esculentus* starch powder. Optical rotation of *C. esculentus* starch was determined by a polarimeter (W22-1S, Suoguang Optoelectronic Technology Co., Ltd., Shanghai, China). The starch extraction yield was calculated as follows,

$$\text{Starch purity (\%)} = \frac{\alpha \times 10^6}{L \times W \times 203 \times (100\text{-}H)} \times 100 \quad (1)$$

$$\text{Starch extraction yield (\%)} = \frac{M_1 \times P_1}{M_2 \times P_2} \times 100 \quad (2)$$

where α is the optical rotation of starch, L (dm) is the length of the optical rotation tube, W (g) is the quantity of starch, H (%) denotes the moisture content of starch, M_1 (g) and P_1 (%) are the quality and purity of *C. esculentus* starch, respectively, and M_2 (g) and P_2 (%) are the quality and purity of *C. esculentus* defatted powder, respectively.

Single-Factor Test

Only one factor was changed at a time, while other factors remained unchanged (pH value of 10, ultrasound temperature of 45 ℃, ultrasound time of 30 min, solid-liquid ratio of 1:9). The factor levels were set as ultrasound time (10, 20, 30, 40, 50, and 60 min), pH value (8, 9, 10, 11, 12, and 13), ultrasound temperature (water bath temperature during ultrasound, set to 30, 35, 40, 45, 50, and 55 ℃), and solid-liquid ratio (1:5, 1:7, 1:9, 1:11, 1:13, and 1:15), with starch extraction yield as the evaluation index.

Box-Behnken Design

According to the Box-Behnken design (BBD) of response surface methodology (RSM), three points around the optimal level of factors were selected based on the results of the single-factor test. The starch extraction yield was taken as the evaluation index, and a four factor, three level of BBD was performed using Design Expert 8.0 software. The experimental level and coding are shown in Table 1.

Table 1. Factor Levels and Encoding of Box-Behnken Design

Level	Factor			
	A: Ultrasound Time (min)	B: pH	C: Ultrasound Temperature (°C)	D: Solid-liquid Ratio
-1	20	8	40	1: 9
0	30	9	45	1:11
1	40	10	50	1:13

SEM

For capturing scanning electron micrographs (JSM-6490 SEM, JEOL, Peabody, MA, USA), a small amount of starch sample was added onto double-sided conductive adhesive and dispersed into a thin layer. An ion sputtering instrument was used to spray platinum on the surface of the sample for approximately 1.0 mm, with a voltage of 3 kV and an amplification factor of 3000X.

RVA

A rapid viscosity analyzer (RVA 4800, Perten, Sweden) was used to analyze the viscosity change curves of four types of starch during gelatinization and retrogradation processes. The operation method and testing procedure of RVA are based on GB/T 24853 (2010). Approximately 25 mL of water was taken and placed in a sample cylinder. A total of 3 g of starch (corrected on a 14% wet basis) was accurately added in the cylinder, gently stirred well, and placed in a rapid viscosity analyzer to measure the viscosity change curve of the sample.

DSC

A differential scanning calorimeter (TA Q20, Perkin Elmer Limited, Hopkinton, MA, USA) was used to determine the thermal stability of starch. Approximately 2.5 mg of starch and 7.5 μL distilled water were added into an aluminum plate in proper order. It was allowed to equilibrate at room temperature for 24 h. The scanning temperature range was 30 to 120 ℃, and the heating rate was 10 ℃/min.

Swelling Power and Solubility

The determination of starch swelling power and solubility was based on a modified method of Akonor *et al.* (2019). About 150 mg of starch and 10 mL of distilled water were added into a centrifuge tube. The tube was vortex mixed (Vortex 6, Kylin-Bell, Jiangsu, China) and reciprocating vibrated for 30 min in a water bath shaker (250 r/min, SHA-C, Zhiborui Instrument Manufacturing Co., Ltd., Jiangsu, China) at temperatures of 25 ℃, 60 ℃, and 85 ℃, respectively. The sample was allowed to cool to room temperature, and the tube was centrifuged at 4000 r/min for 40 min. The centrifuged supernatant was poured into a dry aluminum box and dried at 130 ℃ to a constant weight. The sediment quality and the quantity change of the aluminum box were weighed.

$$\text{Solubility (\%)} = \frac{\text{Weight of dissolved starch}}{\text{Sample weight}} \times 100 \quad (3)$$

$$\text{Swelling power (g/g)} = \frac{\text{Weight of swollen granules}}{\text{Weight of sample–Weight of dissolved starch}} \quad (4)$$

Statistical Analysis

The Design Expert 8.0 software (Stat-Ease, Inc, Minneapolis, MN, USA) was used for the BBD experiment and data analysis. All experiments were performed twice or more. The final results were evaluated using the statistical analysis software IBM SPSS Statistics 21 (IBM Corp., Armonk, NY, USA). The significant levels were established at $p < 0.05$. Statistical analysis was performed using the software Origin 2018 (Origin Lab Co., Northampton, MA, USA).

RESULTS AND DISCUSSION

The Influence of Single Factors on Starch Extraction Yield

The results of the single-factor test are shown in Fig. 1. The effects of four factors, namely ultrasound time, pH, ultrasound temperature, and solid-liquid ratio, on the starch extraction yields from *C. esculentus* were studied. As shown in Fig. 1A, when the ultrasound time was 10 to 30 min, the starch extraction yield increased with the prolongation of ultrasound time, indicating that ultrasound had a promoting effect on starch extraction. Extraction yield began to decrease at 30 to 60 min, which may indicate that excessive ultrasound treatment damaged the structure of starch particles. The effect of ultrasound on starch structure and mechanical effects generated by ultrasound cavitation could degrade starch particles (BeMiller and Huber 2015).

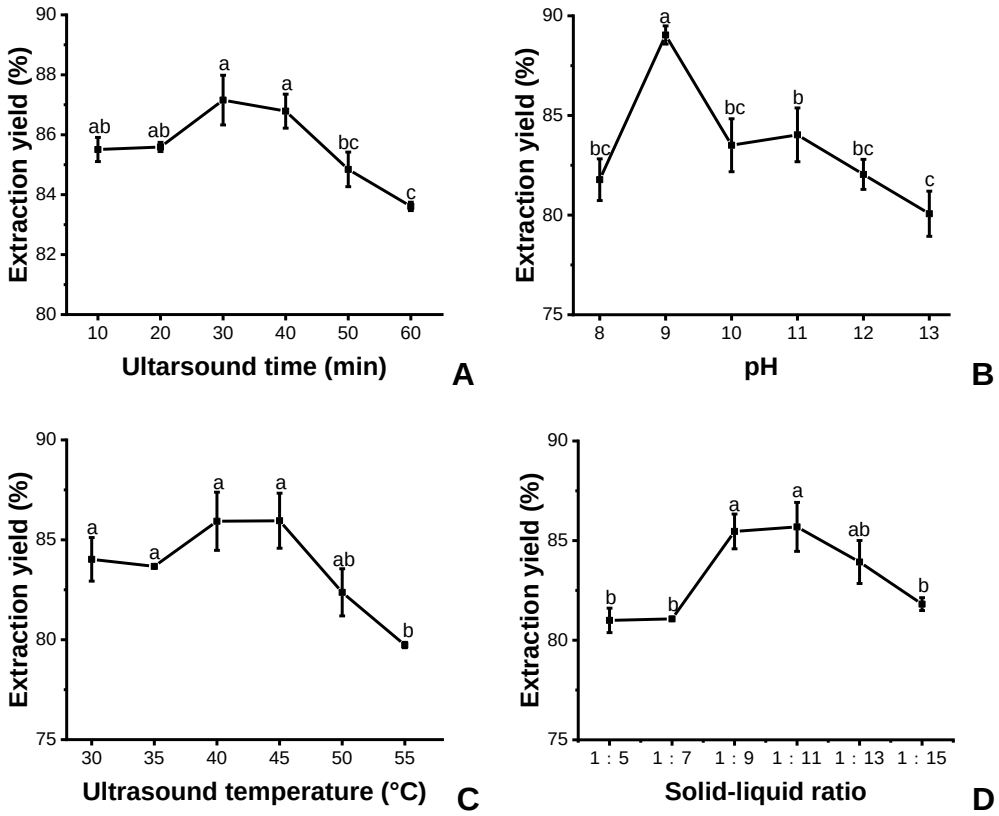

Fig. 1. Single-factor test results (Error bars are used to represent the magnitude of uncertainty, and the height of the error bar is ± standard error)

Figure 1B shows that the optimal extraction effect was achieved when the pH of the alkaline solution was 9. However, as the OH^- concentration continues to increase, starch is hydrolyzed, leached, and oxidized, leading to a decrease in extraction yield (Karim *et al.* 2008). Figure 1C shows the effect of temperature on starch extraction yield. As the temperature increased, the starch yield showed an upward trend. However, when the temperature exceeded 45 ℃, the yield began to decrease. Perhaps the decrease in extraction rate is due to the swelling of starch particles, making it difficult to separate from components such as fibers and proteins (Ozturk *et al.* 2021). Figure 1D shows that the optimal solid-liquid ratio was 1:11. Insufficient addition of alkaline solution could not fully dissolve the protein, while excessive addition of alkaline solution might enhance the hydrolysis of starch.

Optimization of Starch Extraction

The Box-Behnken experiment and results are shown in Table 2.

Table 2. Box-Behnken Design Experiment and Results

Number	Ultrasound Time (min) (A)	pH (B)	Ultrasound Temperature (°C) (C)	Solid-liquid Ratio (D)	Extraction Yield (%)
1	20	8	45	11	86.10
2	40	8	45	11	85.29
3	20	10	45	11	87.38
4	40	10	45	11	86.15
5	30	9	40	9	91.32
6	30	9	50	9	87.73
7	30	9	40	13	88.80
8	30	9	50	13	86.91
9	20	9	45	9	87.05
10	40	9	45	9	87.39
11	20	9	45	13	86.35
12	40	9	45	13	85.31
13	30	8	40	11	88.35
14	30	10	40	11	87.91
15	30	8	50	11	87.10
16	30	10	50	11	87.80
17	20	9	40	11	87.56
18	40	9	40	11	89.38
19	20	9	50	11	87.47
20	40	9	50	11	86.17
21	30	8	45	9	86.29
22	30	10	45	9	87.77
23	30	8	45	13	87.30
24	30	10	45	13	86.60
25	30	9	45	11	89.81
26	30	9	45	11	89.69
27	30	9	45	11	89.67
28	30	9	45	11	88.47
29	30	9	45	11	88.57

Design Expert software was used to fit the quadratic multiple regression equation between ultrasound time (A), pH value (B), ultrasound temperature (C), solid-liquid ratio (D), and starch extraction yield:

$$\text{Extraction yield (\%)} = 89.24 - 0.19A + 0.27B - 0.84C - 0.52D - 0.10AB - 0.78AC - 0.35AD + 0.28BC - 0.55BD + 0.43CD - 1.73A^2 - 1.43B^2 + 0.13C^2 - 0.83D^2$$

From Table 3, it can be seen that the P-value of the model was extremely significant, while the lake-of-fit was not significant. Among the four influencing factors, ultrasound temperature had an extremely significant impact on extraction yield, solid-liquid ratio had a significant impact, and ultrasound time and pH value had no significant impacts on extraction yield. From the F values of the four factors and the coefficients of the regression equation, the order of influence on starch yield was: ultrasound temperature > solid-liquid ratio > pH value > ultrasound time. The R^2 of the model was 0.8768, indicating that the model could explain the experimental results well. The coefficient of variation (CV) was 0.81%, and a small CV value indicated that the regression equation had a good fit. The signal-to-noise ratio was 9.263, which was greater than four, indicating that the model was reliable.

Through the analysis and optimization of Design Expert 8.0, the optimal process conditions were obtained, which were ultrasound time of 32.32 min, pH value of 9.11, ultrasound temperature of 40 ℃, and solid-liquid ratio of 9.69:1. The predicted extraction percentage under these conditions was 90.60%. To verify the reliability of these results, an actual extraction of 90.08 ± 0.48 (%) was obtained by selecting an ultrasound time of 30 min, pH value of 9.00, ultrasound temperature of 40 ℃, and a solid-liquid ratio of 10:1. The obtained result was close to the predicted values, and the plan was judged to be feasible.

Table 3. Box-Behnken Design Analysis of Variance

Source of Variance	Sum of Squares	Degree of Freedom	Mean Square	F-value	P-value	Significance
model	49.86	14	3.56	7.12	0.0004	**
A-Ultrasound time	0.42	1	0.42	0.83	0.3773	
B-pH	0.84	1	0.84	1.69	0.2152	
C-ultrasound temperature	8.54	1	8.54	17.07	0.001	**
D-Solid-liquid ratio	3.28	1	3.28	6.56	0.0226	*
AB	0.043	1	0.043	0.087	0.7728	
AC	2.42	1	2.42	4.84	0.0451	*
AD	0.49	1	0.49	0.97	0.3415	
BC	0.32	1	0.32	0.64	0.4356	
BD	1.19	1	1.19	2.38	0.1453	
CD	0.72	1	0.72	1.45	0.2488	
A^2	19.48	1	19.48	38.93	0.0001	**
B^2	13.23	1	13.23	26.43	0.0001	**
C^2	0.11	1	0.11	0.22	0.6483	
D^2	4.47	1	4.47	8.94	0.0098	**
Residual	7.00	14	0.5			
Lake-of-fit	5.24	10	0.52	1.18	0.4719	
Pure error	1.77	4	0.44			
Total deviation	56.86	28				
** Significant at the 0.01 level * Significant at the 0.05 level						

The power of the ultrasound instrument is 200 W, and the electrical energy consumption for 30 min is 0.1 kWh. This device has a capacity of 10 L and theoretically can handle up to approximately 1 kg of *C. esculentus* powder. The energy consumption of 1 t of *C. esculentus* powder is estimated to be 100 kWh.

Microstructure of Starch Granules

The SEM images in Fig. 2 indicate that the microstructure of *C. esculentus* starch was similar to potato starch and cassava starch, with smooth circular or elliptical particles on the surface. *Cyperus esculentus* starch has a similar appearance to tropical tuber starch such as sweet potato starch (Zhu and Wang 2014; Akonor *et al.* 2019). Cassava starch also contains many truncated granules (Waterschoot *et al.* 2015). The shape of corn starch was significantly different from the other three types of starch, presenting a polygonal or irregular shape.

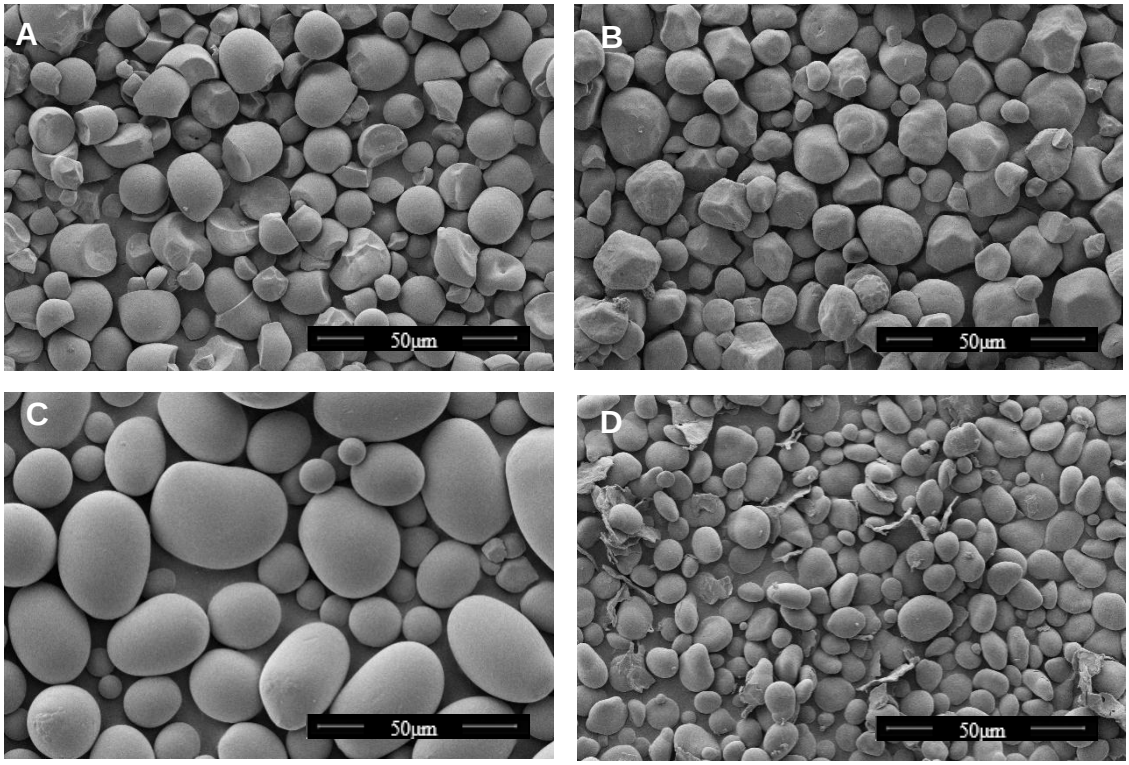

Fig. 2. Scanning electron microscope photographs of starch (A: Cassava; B: Corn; C: Potato; D: *C. esculentus*)

In terms of starch particle size, potato starch had the largest particle size among these types of starch, and its long axis size can reach up to 50 μm. There are reports indicating that the particle size distribution range of potato starch is large, ranging from 5 to 100 μm (Tester *et al.* 2004). In the pictures, the particle sizes of cassava starch and corn starch were relatively close. According to reports, the particle size of corn starch ranged from 5 to 20 μm. The particle size of *C. esculentus* starch was approximately 2 to 15 μm, it could be divided into small and medium-sized starch (Lindeboom *et al.* 2004).

Pasting Properties

The pasting properties of starch are one of the most explored aspects. Starch suspension undergoes particle expansion and rupture, polysaccharide leaching, and viscosity increase with starch gelatinization at a certain temperature (Juhász and Salgó 2008; Balet *et al.* 2019). The RVA curves of cassava, potato, corn, and *C. esculentus* starch suspensions at a concentration of 9.2% are shown in Fig. 3. The corresponding characteristic values of the RVA curves are shown in Table 4. The pasting temperature refers to the temperature at which the viscosity begins to rise. The pasting temperature of rhizome starch is lower than that of grain starch (Jane *et al.* 1999; Kaur *et al.* 2007). The *C. esculentus* starch had a higher pasting temperature than potato starch and cassava starch. The peak viscosity of *C. esculentus* starch was very close to that of cassava starch. Corn starch had the lowest peak viscosity. Reports have shown that the viscosity of grain starch is often low due to its low swelling force (Zhu and Corke 2011; Mieles-Gómez *et al.* 2023).

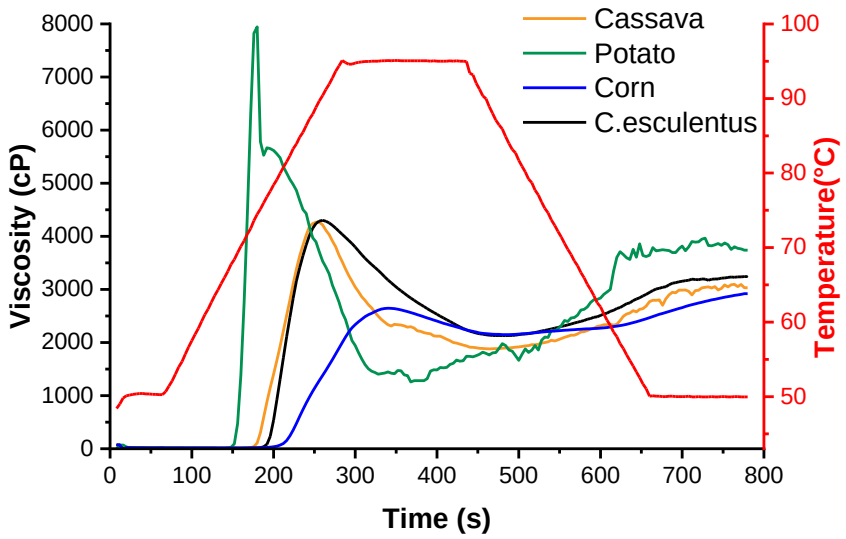

Fig. 3. RVA curve of 9.2% starch suspension

After reaching its maximum, the viscosity of starch began to decrease, which is attributed to the melting of the starch crystallization zone and the rapid entry of water into the particles (Balet *et al.* 2019). The collapse value represents the difference between peak viscosity and valley viscosity. A high collapse value usually indicates poor thermal stability. The viscosity of *C. esculentus* starch decreased more slowly than cassava, and its collapse value was also lower.

During the cooling stage, the four types of starch exhibited varying degrees of retrogradation, which is mainly reflected by their setback value and final viscosity. In the short term, retrogradation is mainly related to the recrystallization of amylose (Chen *et al.* 2015; Fu *et al.* 2017). From Fig. 3, the set-back trend of potato starch was the most obvious. Corn starch was the least noticeable. *Cyperus esculentus* starch had similar retrogradation values, but higher final viscosity compared to cassava starch.

Table 4. RVA Curve Characteristic Values of Starch

Starch Type	Peak Viscosity (cP)	Valley Viscosity (cP)	Collapse Value (cP)	Final Viscosity (cP)	Set-back Value (cP)	Peak Time (min)	Pasting Temperature (°C)
Cassava	4288 ± 29.70b	1883 ± 2.83b	2405 ± 26.87b	3021.5 ± 14.85c	1138.5 ± 17.68b	4.2 ± 0c	73.55 ± 0.07c
Potato	8036 ± 131.52a	1222.5 ± 48.79c	6813.5 ± 180.31a	3764 ± 33.94a	2541.5 ± 82.73a	2.94 ± 0.09d	68.2 ± 0.57d
Corn	2690 ± 62.23c	2152 ± 4.95a	537.5 ± 57.28d	2994.5 ± 106.77c	842 ± 101.82c	5.64 ± 0.05a	79.95 ± 0.07a
C. esculentus	4235 ± 91.92b	2121 ± 12.73a	2114 ± 79.2c	3206 ± 49.50b	1085 ± 36.77b	4.37 ± 0.05b	76.75 ± 0.07b

Swelling power and solubility

Swelling power and solubility, as parameters for evaluating starch properties, are influenced by various factors, and the distribution and content of amylopectin play a major role, while the presence of amylose acts as a diluent and limits the expansion of starch (Tester *et al.* 1993). The solubility and swelling power of starch at different temperatures are shown in Table 5.

Table 5. Solubility and Swelling Power of Starch at Different Temperatures

Temperature	Cassava Starch	Potato Starch	Corn Starch	*C. esculentus* Starch
Solubility (%)				
25 °C	0.18 ± 0.04b	0.28 ± 0.06ab	0.39 ± 0.08a	0.30 ± 0.15ab
60 °C	1.67 ± 0.13b	4.44 ± 0.09a	0.54 ± 0.11c	0.25 ± 0.09d
85 °C	16.21 ± 0.05a	5.21 ± 0d	8.65 ± 0.13c	13.98 ± 0.66b
Swelling Power (g/g)				
25 °C	2.36 ± 0.14a	2.35 ± 0.02a	2.45 ± 0.21a	2.40 ± 0.09a
60 °C	4.39 ± 0.10b	16.64 ± 0.93a	3.49 ± 0.08c	2.63 ± 0.07c
85 °C	29.24 ± 0.08b	31.46 ± 0.27a	14.14 ± 0.13d	26.67 ± 1.01c

As shown in Table 5, the solubility of all four types of starch was very low at room temperature of 25 ℃, but when the temperature rose to 60 ℃, it began to show differences. The solubility of corn starch and *C. esculentus* starch showed little change and almost no increase at 60 ℃, but cassava and potato starch began to partially dissolve. At 85 ℃, the solubility of *C. esculentus* starch was higher than that of potato and corn starch, but lower than that of cassava starch. Akonor *et al.* (2019) measured the solubility of two types of *C. esculentus* (black and yellow), with a solubility of 11.6 ± 0.3% for black and 13.5 ± 0.2% for yellow. It is generally believed that amylose begins to leach below 70 ℃, while amylopectin only begins to leach above 90 ℃. Therefore, it can be considered that the dissolved component of starch at 60 ℃ and 85 ℃ is mainly amylose (Vandeputte *et al.* 2003; Gomand *et al.* 2010).

As shown in Table 5, the swelling power was relatively close at room temperature, both around 2.4 g/g. However, at 60 ℃, the swelling power of cassava and potato starch was higher than corn and *C. esculentus*. At 85 ℃, the swelling power of corn starch is noticeably lower than that of tuberous starches (Waterschoot *et al.* 2015). At 60 ℃, *C.*

esculentus starch had the lowest swelling power, while at 85 ℃, *C. esculentus* starch exhibited a high swelling power like other tuber starch types.

Gelatinization properties

Gelatinization refers to the irreversible process of starch suspension heating in the presence of excess water, from ordered to disordered nature (Jenkins and Donald 1998). During the gelatinization process, there is a phenomenon of heat absorption and differential scanning calorimeter can measure this heat absorption (Baks *et al.* 2007). As shown in Fig. 4 and Table 6, the peak temperature of *C. esculentus* starch was similar to that of corn and cassava, but the gelatinization temperature range (T_c-T_o) of cassava was larger than both.

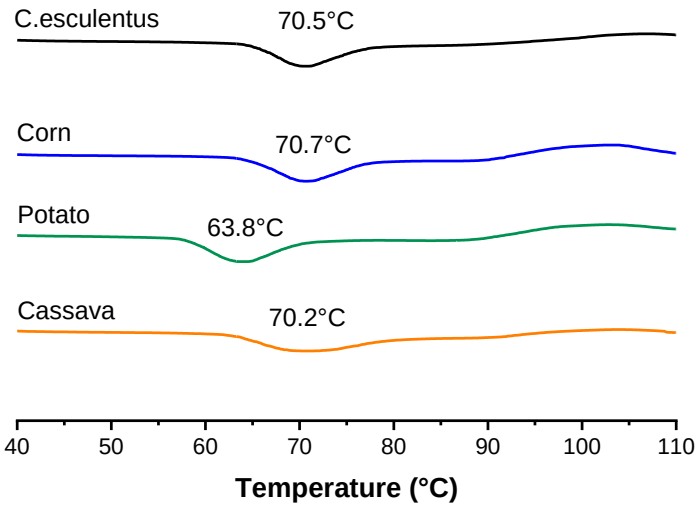

Fig. 4. DSC curves for detecting starch gelatinization characteristics

Table 6. DSC Results of Starch Gelatinization Characteristics

Starch Type	T_o (°C)	T_p (°C)	T_c (°C)	Δ H (J/g)
Cassava	59.72 ± 0.86b	70.19 ± 0.27a	82.94 ± 0.37a	12.85 ± 0.20a
Potato	56.24 ± 0.75c	63.83 ± 0.33b	74.76 ± 0.13d	13.70 ± 0.81a
Corn	62.91 ± 0.42a	70.65 ± 0.35a	81.58 ± 0.21b	12.88 ± 1.12a
C. esculentus	62.05 ± 0.49a	70.53 ± 0.19a	80.56 ± 0.27c	12.76 ± 0.95a

CONCLUSIONS

1. Compared with the other three types of starch, *Cyperus esculentus* starch had good pasting properties such as high peak viscosity and low collapse value. *C. esculentus* starch had high swelling power and solubility at 85 ℃ and good food and industrial prospects.
2. The starch from *C. esculentus* was not easily separated from oil, and there was no mature industrial method for *C. esculentus* starch extraction. Ultrasound-assistance can improve the efficiency of starch extraction.
3. After optimizing the conditions of ultrasound-assisted extraction, the optimal yield of

C. esculentus starch was obtained as 90.1%. The microstructure results showed that *C. esculentus* starch had a small to medium-sized particle size. The gelatinization temperature of *C. esculentus* starch was 70.5 °C

ACKNOWLEDGMENTS

This research has been funded by the Open Project Program of National Engineering Research Center of Wheat and Corn Further Processing in Henan University of Technology (No. NL2022012), the Cultivation Programme for Young Backbone Teachers in Henan Province (2021GGJS059), and funded by Natural Science Innovation Fund Support Program from Henan University of Technology (2021ZKCJ12).

REFERENCES CITED

Akonor, P. T., Tortoe, C., Oduro-Yeboah, C., Saka, E. A., and Ewool, J. (2019). "Physicochemical, microstructural, and rheological characterization of tiger nut *(Cyperus esculentus)* starch," *International Journal of Food Science* 2019, article ID 3830651. DOI: 10.1155/2019/3830651

Adel, A. A., Awad, A. R., Mohamed, H. H., and Iryna, S. (2015). "Chemical composition, physicochemical properties and fatty acid profile of tiger nut (*Cyperus esculentus* L) seed oil as affected by different preparation methods-all databases," *International Food Research Journal* 22, 1931-1938.

Aydar, E. F., Sena, T., and Beraat, O. (2020). "Plant-based milk substitutes: bioactive compounds, conventional and novel processes, bioavailability studies, and health effects," *Journal of Functional Foods* 70, article ID 103975. DOI: 10.1016/j.jff.2020.103975.

Baks, T., Ngene, I. S., Van Soest, J. J. G., Janssen, A. E. M., and Boom, R. M. (2007). "Comparison of methods to determine the degree of gelatinisation for both high and low starch concentrations," *Carbohydrate Polymers* 67(4), 481-490. DOI: 10.1016/j.carbpol.2006.06.016

Balet, S., Guelpa, A., Fox, G., and Manley, M. (2019). "Rapid visco analyser (RVA) as a tool for measuring starch-related physiochemical properties in cereals: A review," *Food Analytical Methods* 12(10), 2344-2360. DOI: 10.1007/s12161-019-01581-w

BeMiller, J. N., and Huber, K. C. (2015). "Physical modification of food starch functionalities," *Annual Review of Food Science and Technology* 6(1), 19-69. DOI: 10.1146/annurev-food-022814-015552

Chukwuma, E. R., Obioma, N. U., and Christopher, O. I. (2010). "The phytochemical composition and some biochemical effects of Nigerian tigernut (*Cyperus esculentus* L.) tuber," *Pakistan Journal of Nutrition* 9, 709-715.

Cárcel, J. A., García-Pérez, J. V., Benedito, J., and Mulet, A. (2012). "Food process innovation through new technologies: Use of ultrasound," *Journal of Food Engineering* 110(2), 200-207. DOI: 10.1016/j.jfoodeng.2011.05.038

Chen, L., Ren, F., Zhang, Z., Tong, Q., and Rashed, M. M. A. (2015). "Effect of pullulan on the short-term and long-term retrogradation of rice starch," *Carbohydrate Polymers* 115, 415-421. DOI: 10.1016/j.carbpol.2014.09.006

Codina-Torrella, I., Buenaventura, G., and Antonio, J. T. (2015). "Characterization and comparison of tiger nuts (*Cyperus esculentus L.*) from different geographical origin," *Industrial Crops and Products* 65, 406-414. DOI: 10.1016/j.indcrop.2014.11.007.

Fu, Z., and BeMiller, J. N. (2017). "Effect of hydrocolloids and salts on retrogradation of native and modified maize starch," *Food Hydrocolloids* 69, 36-48. DOI: 10.1016/j.foodhyd.2017.01.023

GB/T 24853 (2010). "General pasting method for wheat or rye flour or starch – Using the rapid visco analyzer," Standardization Administration of China, Beijing, China.

Gomand, S. V., Lamberts, L., Visser, R. G. F., and Delcour, J. A. (2010). "Physicochemical properties of potato and cassava starches and their mutants in relation to their structural properties," *Food Hydrocolloids* 24(4), 424-433. DOI: 10.1016/j.foodhyd.2009.11.009

Jane, J., Chen, Y. Y., Lee, L. F., McPherson, A. E., Wong, K. S., Radosavljevic, M., and Kasemsuwan, T. (1999). "Effects of amylopectin branch chain length and amylose content on the gelatinization and pasting properties of starch," *Cereal Chemistry* 76(5), 629-637. DOI: 10.1094/CCHEM.1999.76.5.629

Jenkins, P. J., and Donald, A. M. (1998). "Gelatinisation of starch: A combined SAXS/WAXS/DSC and SANS study," *Carbohydrate Research* 308(1–2), 133-147. DOI: 10.1016/S0008-6215(98)00079-2

Juhász, R., and Salgó, A. (2008). "Pasting behavior of amylose, amylopectin and their mixtures as determined by rva curves and first derivatives," *Starch - Stärke* 60(2), 70-78. DOI: 10.1002/star.200700634

Karim, A. A., Nadiha, M. Z., Chen, F. K., Phuah, Y. P., Chui, Y. M., and Fazilah, A. (2008). "Pasting and retrogradation properties of alkali-treated sago (*Metroxylon sagu*) starch," *Food Hydrocolloids* 22(6), 1044-1053. DOI: 10.1016/j.foodhyd.2007.05.011

Kaur, A., Singh, N., Ezekiel, R., and Guraya, H. S. (2007). "Physicochemical, thermal and pasting properties of starches separated from different potato cultivars grown at different locations," *Food Chemistry* 101(2), 643–651. DOI: 10.1016/j.foodchem.2006.01.054

Lindeboom, N., Chang, P. R., and Tyler, R. T. (2004). "Analytical, biochemical and physicochemical aspects of starch granule size, with emphasis on small granule starches: A review," *Starch - Stärke* 56(3–4), 89-99. DOI: 10.1002/star.200300218

Manek, R. V., Builders, P. F., Kolling, W. M., Emeje, M., and Kunle, O. O. (2012). "Physicochemical and binder properties of starch obtained from *Cyperus esculentus*," *AAPS PharmSciTech* 13(2), 379-388. DOI: 10.1208/s12249-012-9761-z

Mieles-Gómez, L., Quintana, S. E., and García-Zapateiro, L. A. (2023). "Ultrasound-assisted extraction of mango (*Mangifera indica*) kernel starch: Chemical, techno-functional, and pasting properties," *Gels* 9(2), article 136. DOI: 10.3390/gels9020136

Ozturk, O. K., Kaasgaard, S. G., Palmén, L. G., Vidal, B. C., and Hamaker, B. R. (2021). "Enzyme treatments on corn fiber from wet-milling process for increased starch and protein extraction," *Industrial Crops and Products* 168, article ID 113622. DOI: 10.1016/j.indcrop.2021.113622

Sánchez-Zapata, E., Fernández-López, J., and Angel Pérez-Alvarez, J. (2012). "Tiger nut (*Cyperus esculentus*) commercialization: Health aspects, composition, properties, and food applications," *Comprehensive Reviews in Food Science and Food Safety* 11(4), 366-377. DOI: 10.1111/j.1541-4337.2012.00190.x

Tester, R. F., and Morrison, W. R. (1993). "Swelling and gelatinization of cereal starches. VI. Starches from waxy hector and hector barleys at four stages of grain development," *Journal of Cereal Science* 17(1), 11-18. DOI: 10.1006/jcrs.1993.1002

Tester, R. F., Karkalas, J., and Qi, X. (2004). "Starch—Composition, fine structure and architecture," *Journal of Cereal Science* 39(2), 151-165. DOI: 10.1016/j.jcs.2003.12.001

Vandeputte, G. E., Derycke, V., Geeroms, J., and Delcour, J. A. (2003). "Rice starches. II. Structural aspects provide insight into swelling and pasting properties," *Journal of Cereal Science* 38(1), 53-59. DOI: 10.1016/S0733-5210(02)00141-8

Wang, N., Shi, N., Fei, H., Liu, Y., Zhang, Y., Li, Z., Ruan, C., and Zhang, D. (2022). "Physicochemical, structural, and digestive properties of pea starch obtained *via* ultrasonic-assisted alkali extraction," *Ultrasonics Sonochemistry* 89, article ID article 106136. DOI: 10.1016/j.ultsonch.2022.106136

Waterschoot, J., Gomand, S. V., Fierens, E., and Delcour, J. A. (2015). "Production, structure, physicochemical and functional properties of maize, cassava, wheat, potato and rice starches," *Starch - Stärke* 67(1–2), 14-29. DOI: 10.1002/star.201300238

Wu, Z. W., Huang, H. R., Liao, S. Q., Cai, X. S., Liu, H. M., Ma, Y. X., and Wang, X. D. (2024). "Evaluation of quality properties of brown tigernut (*Cyperus esculentus L.*) tubers from six major growing regions of China: A new source of vegetable oil and starch." *Journal of Oleo Science* 73(2), 147-161. DOI: 10.5650/jos.ess23123.

Yu, T., Wu, Q., Wang, J. M., Lang, B., Wang, X. S., and Shang, X. Z. (2023). "Physicochemical properties of tiger nut (*Cyperus esculentus* L) polysaccharides and their interaction with proteins in beverages." *Food Chemistry-X* 19, article ID 100776. DOI: 10.1016/j.fochx.2023.100776.

Zhu, F., and Corke, H. (2011). "Gelatinization, pasting, and gelling properties of sweet potato and wheat starch blends," *Cereal Chemistry* 88(3), 302-309. DOI: 10.1094/CCHEM-10-10-0145

Zhu, F., and Wang, S. (2014). "Physicochemical properties, molecular structure, and uses of sweet potato starch," *Trends in Food Science & Technology* 36(2), 68-78. DOI: 10.1016/j.tifs.2014.01.008

Article submitted: March 5, 2024; Peer review completed: April 13, 2024; Revised version received: April 18, 2024; Accepted: May 4, 2024; Published: May 9, 2024.
DOI: 10.15376/biores.19.3.4264-4277